

Instantaneous ionization rate of H_2^+ in intense laser field; Interpretation of the Enhanced Ionization

Mohsen Vafae¹, Hassan Sabzyan¹, Zahra Vafae¹, Ali Katanforoush²

¹ Department of Chemistry, University of Isfahan, Isfahan 81746-73441, I. R. Iran

² School of Mathematics, Institute for Studies in Theoretical Physics and Mathematics (IPM), Tehran 19395-5746, I. R. Iran

E-mail: mohsenvafae@gmail.com, sabzyan@sci.ui.ac.ir

Abstract

The fixed-nuclei full dimensional time-dependent Schrödinger equation is directly solved for H_2^+ in the linearly polarized laser field of $I=1.0 \times 10^{14}$ W/cm² and $\lambda = 1064$ nm. Instantaneous ionization rate has been introduced and calculated by evaluating the instantaneous imaginary energy of the system. It is shown that positive (negative) values of instantaneous imaginary energy of the system represent the incoming (outgoing) instantaneous current of electron. This approach allows us to determine not only the instantaneous intensity but also the instantaneous direction of the electronic current. The instantaneous behavior of the electron wavepacket in intense laser field can thus be probed precisely. Details of the enhanced ionization rates are studied based on the instantaneous ionization rates. This approach gives direct evidence for existence of the effect of charge-resonance-enhanced multiphoton resonances of the quasienergy states (QES) with excited electronic states at some particular internuclear distances. Finally, Contributions of the individual time dependent Floquet QES to the overall ionization rates are evaluated.

Introduction

Hydrogen atom and hydrogen molecular ion are two fundamental and prototypical systems which can be used to understand and extend the science of atomic and molecular physics. In intense laser field, these two apparently simple systems exhibit various complex phenomena [1-3]. An interesting and complicated effect is the enhancement of the ionization rate of H_2^+ as a function of inter-nuclear separation which results in maxima at some critical inter-nuclear H-H separations. Indirect [4,5] and direct [6] evidences has been reported for a similar behavior in more complex molecules. In order to characterize and interpret this enhanced ionization rates, which was observed previously at some critical inter-nuclear distances [7-12], recent theoretical studies on the H_2^+ -laser interaction have been concentrated on the calculation of the ionization rate as a function of inter-nuclear distance R [13-21].

For the molecules subjected to short intense laser pulses, molecular dissociation is accompanied by ionization. At high intensities ($I > 10^{14}$ W/cm²) for which the ionization process is generally faster than the dissociation process, it is possible to study molecular ionization processes independently at fixed inter-nuclear separations. The ionization rate of H_2^+ near the equilibrium inter-nuclear separation of 2 au is relatively small and thus dissociation proceeds more easily than ionization does. The molecules in intense laser fields are strongly aligned due to the acquired torque from the laser field. Moreover, the ionization process is relatively fast compared to the vibrational motion of the nuclei. Therefore, the numerical solution of the full dimensional time-dependent Schrödinger equation (TDSE) of H_2^+ system in intense laser field is reduced to the numerical solution of the electronic TDSE as the fixed nuclei approximation, which is also experimentally well acceptable, can well be employed.

In this study, ionization of the hydrogen molecular ion H_2^+ under intense linearly polarized pulse of laser fields is simulated by direct solution of the fixed-nuclei, full dimensional electronic TDSE equation for $\lambda = 1064$ nm wavelength and $I=1.0 \times 10^{14}$ W/cm² intensity. Time-dependent Schrödinger equation in the cylindrical polar coordinate system for H_2^+ molecular ion located in the laser field of $E(t) = E_0 f(t) \cos(\omega t)$ parallel to the z axis (inter-nuclear axis) reads as

$$i \frac{\partial \psi(z, \rho, t)}{\partial t} = H(z, \rho, t) \psi(z, \rho, t), \quad (1)$$

where the total 3D electronic Hamiltonian is given by [15,17]

$$H(z, \rho, t) = -\frac{2m_p + m_e}{4m_p m_e} \left[\frac{\partial^2}{\partial \rho^2} + \frac{1}{\rho} \frac{\partial}{\partial \rho} + \frac{\partial^2}{\partial z^2} \right] + V_c(z, \rho, t) \quad (2)$$

$$V_c(z, \rho, t) = \frac{-1}{\left((z \pm R/2)^2 + \rho^2 \right)^{1/2}} + \left(\frac{2m_p + 2m_e}{2m_p + m_e} \right) z E_0 f(t) \cos(\omega t) \quad (3)$$

with E_0 being the laser peak amplitude, $\omega = 2\pi\nu$ the angular frequency, and finally $f(t)$ the laser pulse envelope which is set as

$$f(t) = \begin{cases} \frac{1}{2} \left[1 - \cos\left(\frac{\pi t}{\tau_1}\right) \right] & \text{for } 0 \leq t \leq \tau_1 \\ 1 & \text{for } \tau_1 \leq t \leq \tau_1 + \tau_2 \\ \frac{1}{2} \left[1 - \cos\left(\frac{\pi(t - \tau_2 - 2\tau_1)}{\tau_1}\right) \right] & \text{for } \tau_1 + \tau_2 \leq t \leq 2\tau_1 + \tau_2 \end{cases}, \quad (4)$$

with τ_1 being the rising and falling time and τ_2 being the duration of the laser pulse at its full-scale amplitude. In the present calculations, τ_1 and τ_2 are set to 5 and 15 cycles, respectively. More details of our calculations are described in our previous report [17]. Unless otherwise stated, atomic units have been used throughout.

Time-Dependent Ionization Rates; Results and Discussion

We performed the simulation for a huge box, i.e. with (640,170) size for (z, ρ) directions. The absorber regions are set at $-320 \leq z \leq -300$ and $300 \leq z \leq 320$ for the z direction and at $150 \leq \rho \leq 170$ for the ρ direction [17]. Energy of the H_2^+ system in the laser field can be calculated using:

$$E(t) = \int_{\rho=0}^{\rho=150} \int_{z=-300}^{z=300} \psi(z, \rho, t) H(z, \rho, t) \psi^*(z, \rho, t) \rho d\rho dz, \quad (5)$$

The instantaneous energy thus obtained can be decomposed as $E(t) = E_{\text{Re}}(t) + iE_{\text{Im}}(t)$, where $E_{\text{Re}}(t)$ and $E_{\text{Im}}(t)$ are the real and imaginary parts of the instantaneous total energy of the system, respectively.

The imaginary energy was used previously to calculate the ionization rate in the wavepacket method [19] via the $\Gamma = -2E_{\text{Im}}$ relation. This relation has so far been used to calculate ionization rate in the Floquet method, both in the time-independent [13] and time-dependent [18] approaches. Here, we have used the imaginary part of the instantaneous energy for introducing and calculating instantaneous ionization rate, $\Gamma(t)$, as

$$\Gamma(t) = \frac{-2E_{\text{Im}}(t)}{N(t)} \quad (6).$$

in which $N(t)$ is the instantaneous norm of the wavefunction at time t .

Instantaneous imaginary energies of H_2^+ at some fixed inter-nuclear separations have been calculated by direct solution of the time-dependent Schrödinger equation in the presence of the linearly polarized laser field with $I=1.0 \times 10^{14}$ W/cm² and $\lambda = 1064$ nm. The overall ionization rate of H_2^+ at each inter-nuclear distance is calculated by averaging the calculated instantaneous ionization rates. The ionization rates are averaged from $\tau = 10$ to $\tau = 20$ cycles of the laser field. Figure 1 shows the R-dependent ionization rates calculated in the present study (●) for the H_2^+ system. In the same Figure, ionization rates calculated by Lu and Bandrauk (Δ) [15], Peng et al. (\square) [16] and Chu and Chu (\times) [18]

are also given for comparison. The isolated single point on the vertical coordinate at $R=14$ corresponds to the ionization rate of an isolated H atom in the same laser field and is given for comparison. As can be seen from Figure 1, the four sets of calculated ionization rates are in good validating agreement, especially in the range of $R>9.6$. It can be seen also that the first baseline peak (spanning over inter-nuclear distances between $R=4$ and $R=7.5$) is structured. Our results show furthermore a weak peak at $R=4.8$ which is not predicted by previous works, and another stronger peak at $R=6$ which is consistent with Lu and Bandrauk [15] and Chu and Chu [18]. The strongest peak is located at about $R=9.4$.

It is obvious that the instantaneous ionization rate, $\Gamma(t)$, can be obtained by calculating the time-dependent norm of the wavefunction ($N(t) = \|\Psi(t)\|^2$) using

$$\Gamma(t) = \frac{-d \ln(N(t)/N(0))}{dt} \quad (7)$$

where $N(0) = \|\Psi(0)\|^2$ is the norm of the system at $t=0$. Both equations, Eq. (6) and Eq. (7), give the same results.

Evaluation of the instantaneous ionization rate (via either equations) has a distinct advantage; allowing us to follow the time-dependent ionization processes of a system and to study details of the ionization mechanism. For this purpose, the time-dependent ionization rates of H_2^+ in the linearly polarized field of $I= 1.0 \times 10^{14}$ W/cm² intensity and $\lambda = 1064$ nm wavelength for a number of selected inter-nuclear separations have been calculated and presented in Figure 2. The R values in Figure 2 (except for $R=3.6$) correspond to the peaks of the ionization rates presented in Figure 1.

On the basis of Eq. (6), positive (negative) value of instantaneous imaginary energy results in negative (positive) value for instantaneous ionization rate, and therefore, the positive (negative) value of the instantaneous imaginary energy corresponds to the incoming (outgoing) of the electron to (from) the system. For example, as can be seen from Figure 2(a), the instantaneous ionization rate at $R=3.6$,

which are calculated via Eq. (6), has both positive and negative values. The ionization rate at $R=3.6$, $\sim 3.2 \times 10^{-5} \text{ fs}^{-1}$, is negligible because the amplitudes of the variation of the instantaneous ionization rate over time are very small as compared with those at other inter-nuclear separation points (see other parts of Figure 2). Furthermore, the relative outgoing and incoming (returning) electron are nearly equal and thus the cancellation of the two electron currents results in a negligibly small overall ionization rate. The instantaneous ionization rates at inter-nuclear separations other than $R=3.6$ shows that the outgoing current always exceeds the return current, making the overall ionization rate positive (Figure 2).

All of the calculated time-dependent ionization rate curves shown in Figure 2 consist of repeating non-symmetric baseline peaks corresponding to one half cycle of the laser field. Each one of these baseline peaks has several sharp peaks in its structure. The relative amplitudes of these sharp peaks may change, but their relative positions remain almost constant from one baseline peak to the other. The baseline peaks, which are related to the outgoing electron current from the boundary of the system, have a delay time with respect to the peaks of the laser field. For example, our calculation shows that the delay time for $R = 9.6$ is about 0.85 cycle. The delay time depends on the size of the system; the larger the grid size of the system, the longer the delay time.

The mechanism giving rise to the critical distances in which ionization rates are enhanced and details of the R -dependent ionization rates have received considerable attentions from the earliest studies [4-23]. Zuo and Bandrauk [8] suggested that *charge-resonance* and positions of the two lowest levels of the H_2^+ system in the laser field (at its maximum amplitude) can explain the enhanced ionization peaks. Mulyukov et al. [14] believe that *over barrier ionization* out of the higher well for the most prominent peak in the ionization rate is impeded by backscattering of the electron from the hump between the wells. They argued that at certain values of R , the electron can escape more easily by

undergoing a resonant transition to an energetically nearby highly excited state localized in the lower well so that the hump between the wells does not impede over barrier ionization.

Chu and Chu tried to resolve detailed mechanism of the ionization enhancement phenomenon by calculating ionization rates of the QESs [18]. They applied an ac Floquet calculation to study characteristics and dynamical behavior of complex QESs at different R. They introduced a complex-scaling generalized pseudospectral (CSGPS) technique for the determination of the complex QESs for two-center diatomic molecular systems. Chu and Chu's calculations showed that the dominant electron population remains in the $1\sigma_g$ and $1\sigma_u$ states in the laser of $1 \times 10^{14} \text{W/cm}^2$ intensity. Thus, the two distinctly different groups of QESs, i.e. the lower and upper groups, whose major components are the field-free $1\sigma_g$ and $1\sigma_u$, can be derived.

Because of the Floquet symmetry, all of the QESs in the lower (or in the upper) group separated by $2m\omega$ (m is integer) in energy, are in fact physically indistinguishable and contain the same information regarding multiphoton dynamics. Thus, all QESs in the lower (or in the upper) group have identical imaginary energies. They used the dynamical properties of these two sets of QESs to explore the mechanism(s) responsible for the enhanced ionization phenomenon. Their results reported also in Figure 3 indicate that the QESs in the lower and upper groups both show a double-peak enhancement feature. A detailed analysis of the nature and dynamical behavior of these QESs by Chu and Chu [18] reveals that the ionization enhancement is mainly due to the effect of the *charge-resonance-enhanced* multiphoton resonances of the $1\sigma_g$ and $1\sigma_u$ states with the excited electronic states at some particular inter-nuclear distances.

To evaluate individual contribution from the lower and upper sets of QESs to the overall ionization rates, in Figure 3, we have compared the overall ionization rates obtained in the present work (Figure 1) with the isolated ionization rates of these two QESs reported by Chu and Chu [18].

This comparison shows that the lower QES dominantly determines the overall ionization rates for all of the $R < 3.6$ and $R > 5.2$ ranges. While, for the region in between these ranges, i.e. $3.6 < R < 5.2$, both lower and upper QESs contribute competitively to the overall ionization rates. Therefore, the first peak of the R-dependent overall ionization rate curve observed in our calculations can be assigned to the upper QES, and the second and third peaks of the R-dependent overall ionization rate can be attributed to the lower QES.

Based on the instantaneous ionization rate calculated in this work, details of the time-dependent behavior of the system following the variations of the laser field can be extracted and used in the interpretation of the enhanced ionization rates. As can be seen from Figure 2, the enhanced ionization rate at about $R=9.6$ in Figure 1 can be attributed mainly to the several strong and sharp time-dependent ionization peaks. Existence of these strong sharp peaks is a direct evidence for the effect of charge-resonance-enhanced multiphoton resonances of the $1\sigma_g$ and $1\sigma_u$ states with the excited electronic states at some particular inter-nuclear distances [14,18]. These sharp peaks are not necessarily located at the maxima of the laser field oscillations. The baseline peaks at $R=9.6$, Figure 2(d), have large amplitudes without effectively falling to near zero. While at other inter-nuclear distances, baseline peaks of the time-dependent ionization rates fall off effectively to very small values after each rising period (see Figure 2). As compared to $R=9.6$, amplitudes of the baseline peaks at other inter-nuclear separations, for example at $R=6.0$, are relatively small in spite of having some sharp peaks. Therefore, it can be concluded that the overall ionization rate increases as the number of strong sharp peaks and the level of the baseline of the time-dependent ionization rates increase.

Conclusion

In conclusion, we introduced and calculated instantaneous ionization rate based on the instantaneous values of imaginary energy. It is shown that positive and negative instantaneous

imaginary energies of the system represent respectively the incoming (returning) and the outgoing instantaneous current of electron. Thus, the instantaneous behavior of the electron wavepacket in intense laser field can be probed closely using the instantaneous imaginary energy of the system. In this approach, one can determine the instantaneous intensity and direction of the electronic current. We can also determine the delay time of the outgoing electron wavepackets with respect to the corresponding peaks of the laser field. The instantaneous ionization rate is used to study details of the enhanced ionization rates observed at specific inter-nuclear distances. This approach gives direct evidence for the existence of the effect of charge-resonance-enhanced multiphoton resonances of the QESs with excited electronic states at some particular inter-nuclear distances. TDSE and ac Floquet calculations together form a powerful tool to derive detailed mechanism of the ionization enhancement phenomenon. The comparison between the results obtained by these two methods lead us to determine the individual contribution of the QESs to the overall ionization rates.

Acknowledgments

We would like to acknowledge the University of Isfahan for providing financial supports and research facilities. We should also acknowledge Scientific Computing Center of the School of Mathematics, Institute for Studies in Theoretical Physics and Mathematics (IPM) of I. R. Iran for providing High Performance Computing Cluster to carry out calculations.

References:

- [1] A Giusti-Suzor, F H Mies, L F DiMauro, E Charron and B Yang 1995 J. Phys. B, **28**, 309
- [2] J. Posthumus, ed. 2001 **Molecules and Clusters in Intense Laser Field** (Cambridge Univ. Press).
- [3] A. D. Bandrauk, Y. Fujimura, R. J. Gordon, ed. 2002 **Laser Control and Manipulation of Molecules**, (Washington, USA) Amer. Chem. Soc.: Symp. Series 821.
- [4] C. Cornaggia *et al.* 1991 Phys. Rev. A, **44**, 4499
- [5] D. Normand and M. Schmidt 1996 Phys. Rev. A, **53**, R1958
- [6] E. Constant, H. Stapelfeldt, and P. B. Corkum 1996 Phys. Rev. Lett, **76**, 4140
- [7] Codling K. and Frasiniski L. J. 1993 J. Phys. B **26**, 783
- [8] Zuo T. and Bandrauk A. D. 1995 Phys. Rev. A **52**, R2511
- [9] M. Schmidt, D. Normand and C. Cornaggia 1995 J. Phys. Rev. A, **52**, R2511
- [10] Posthumus J. H., Frasiniski L. J., Giles A. J. and Codling K. 1995 J. Phys. B **28**, L349
- [11] Gibson G. N., Li M., Guo C. and Neira J. 1997 Phys. Rev. Lett. **79** 2022
- [12] Williams I. D., McKenna P., Srigengan B., Johnston I. M. G., Bryan W. A., Sanderson J. H., El-Zein A., Goodworth T. R. J., Newell W. R., Taday P. F. and Langley A. J 2000 J. Phys. B: At. Mol. Opt. Phys. **33** 2743
- [13] Madsen L. B., Plummer M. and McCann J. F. 1998 Phys. Rev. A **58**, 456
- [14] Mulyukov Z., Pont M. and Shakeshaft R. 1996 Phys. Rev. A **54**, 4299
- [15] Bandrauk A. D. and Lu H. Z. 2000 Phys. Rev. A, **62**, 053406
- [16] Peng L.-Y., Dundas D., McCann J. F., Taylor K. T. and Williams I. D. 2003 J. Phys. B **36**, L295
- [17] Vafae M. and Sabzyan H. 2004, J. Phys. B, **37**, 4143
- [18] Chu X. and Chu S. I. 2000 Phys. Rev. A, **63**, 013414
- [19] Pont M., Proulx D. and Shakesaft R. 1991 Phys. Rev. A, **44**, 4486

- [20] Telnov D.A. and Chu S. I. 2005 Phys. Rev. A, **71**, 013408
- [21] Sabzyan H. and Vafae M. 2005 Phys. Rev. A, **71**, 063404
- [22] Pavičić D., Kiess A., Hänsch T. W. and Figger H. 2005 Phys. Rev. Lett. **94**, 163002
- [23] Ergler Th., Rudenko A., Feuerstein B., Zrost K., Schröter C. D., Moshhammer R., and Ullrich J. 2005 Phys. Rev. Lett. **95**, 093001

Figure Captions:

Figure 1.

The ionization rate, Γ , of H_2^+ as function of R in the linearly polarized field of $I=1.0\times 10^{14}$ W/cm^2 intensity and $\lambda = 1064$ nm wavelength calculated in this work (\bullet) compared with the calculated ionization rates reported by Lu and Bandrauk (Δ) [15], Peng et al. (\square) [16] and Chu and Chu (\times) [18]. The isolated single point on the vertical coordinate at $R=14$ correspond to the ionization rate of an isolated H atom.

Figure 2.

The instantaneous ionization rates of H_2^+ in the linearly polarized laser field of $I=1.0\times 10^{14}$ W/cm^2 intensity and $\lambda = 1064$ nm wavelength over a two-cycle period, from 14.0 to 16.0 cycles. Note the difference scales used for different R .

Figure 3.

A comparison between the overall ionization rates obtained in this work (\bullet) and individual contributions of the upper and lower quasienergy states (QESs) reported by Chu and Chu [18].

Figure 1

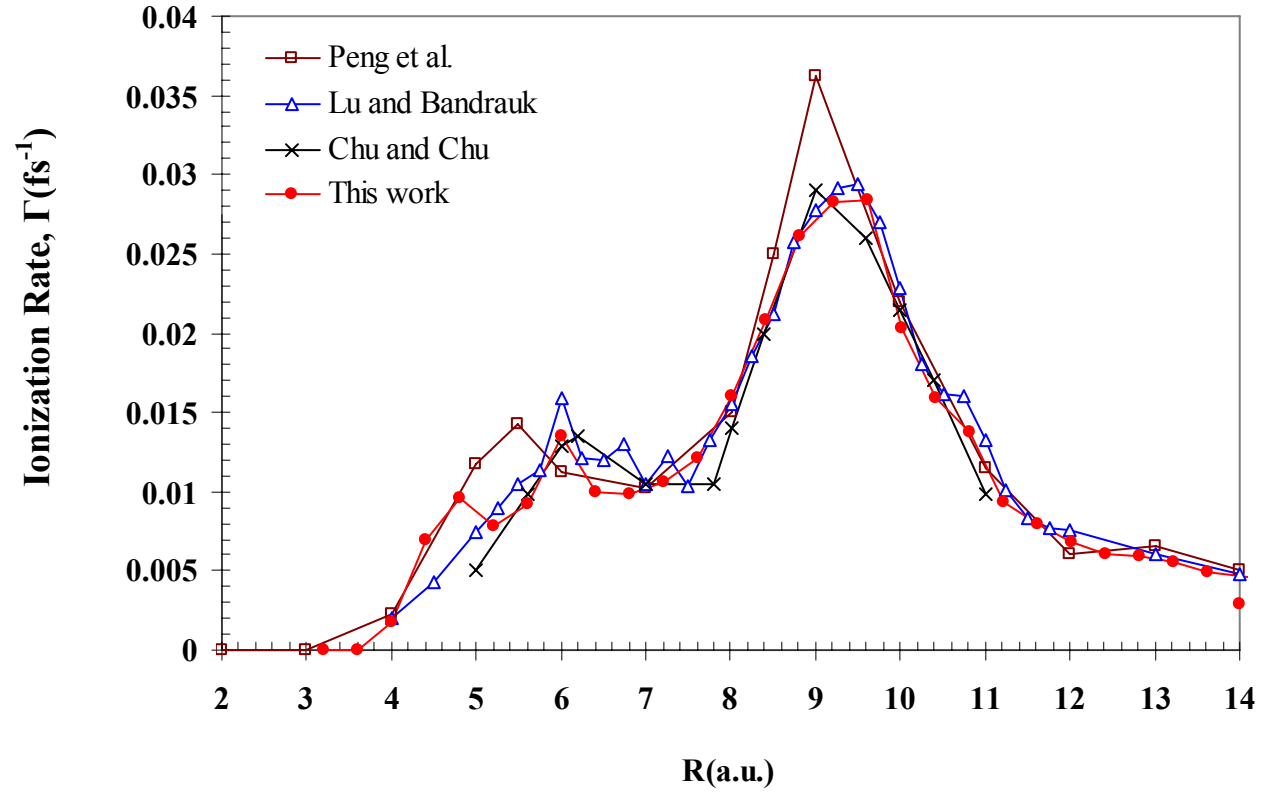


Figure 2

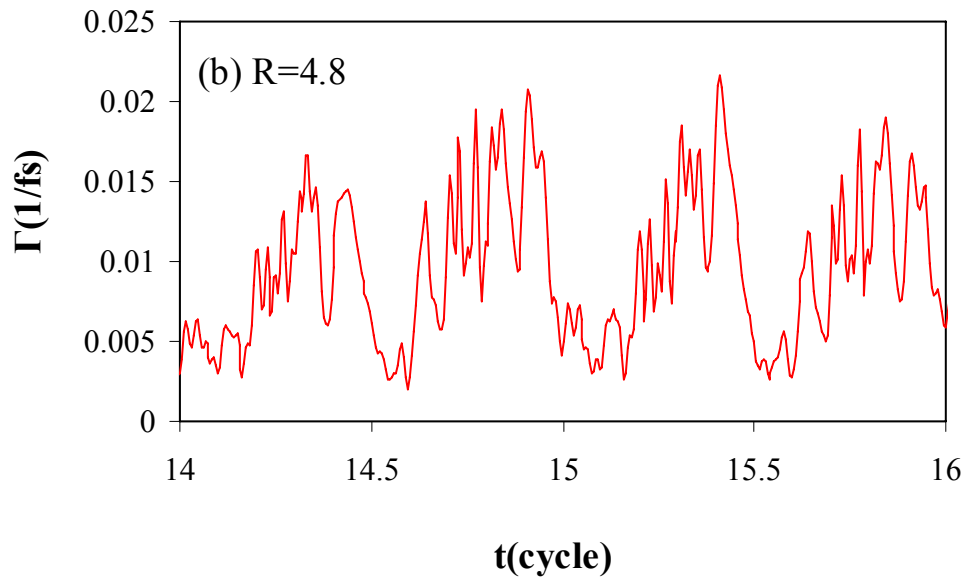
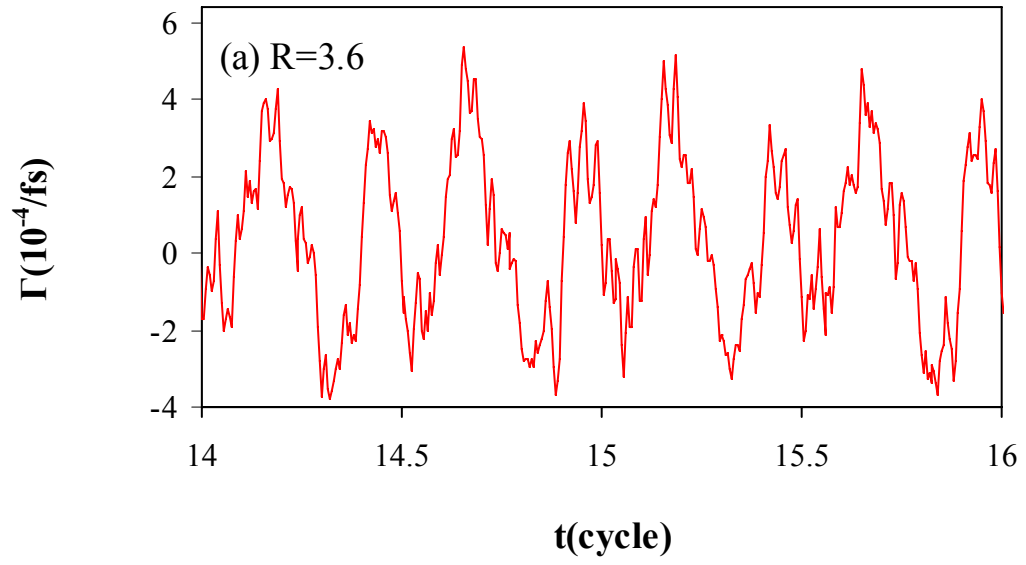


Figure 2 (continued)

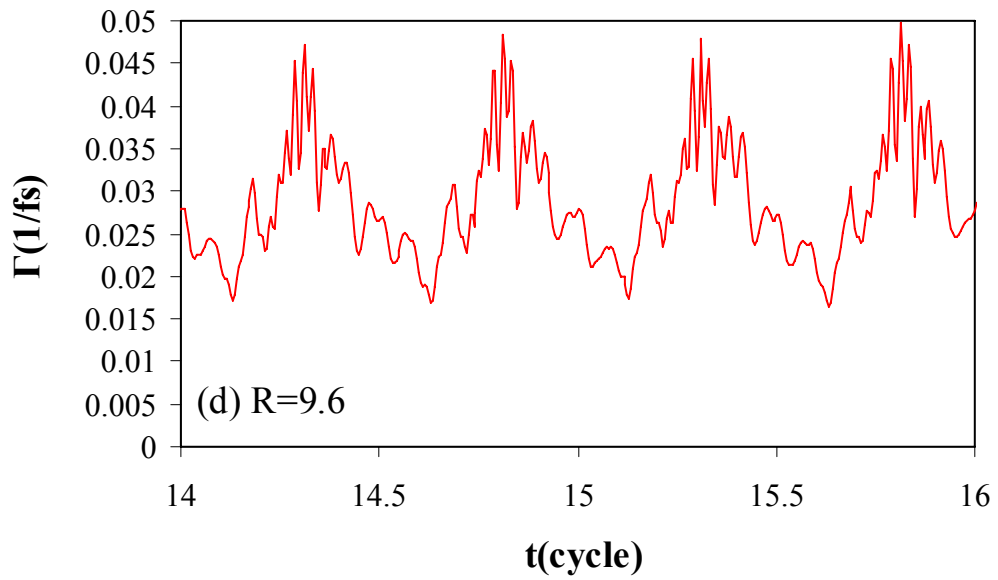
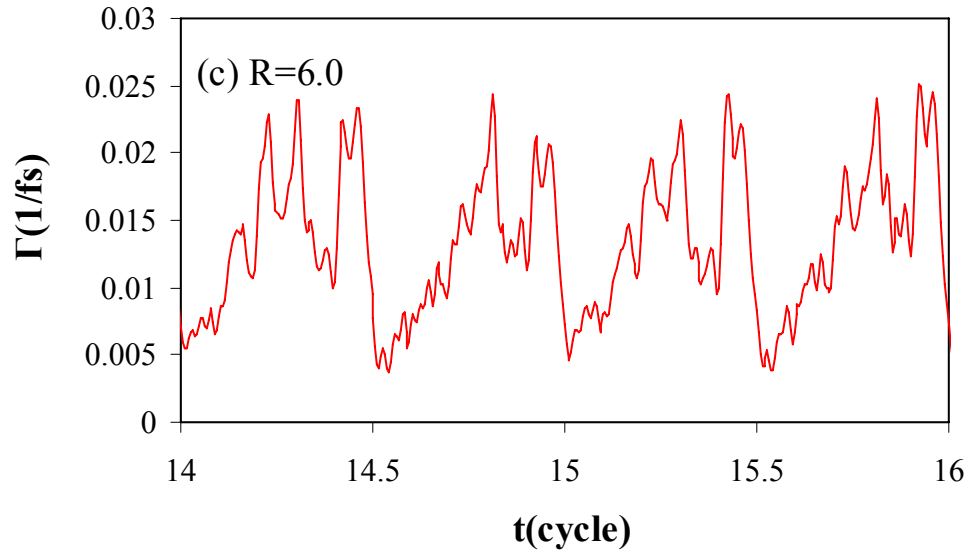


Figure 3

